Magnetic Feshbach resonances in ultracold atom-molecule collisions

Masato Morita [1], Maciej B. Kosicki [2], Piotr S. Żuchowski [3], Paul Brumer [1], and Timur V. Tscherbul [4]

[1]*Chemical Physics Theory Group, Department of Chemistry, and Center for Quantum Information and Quantum Control,*
University of Toronto, Toronto, Ontario, Canada M5S 3H6
[2]*Faculty of Physics, Kazimierz Wielki University, al. Powstańców Wielkopolskich 2, 85-090 Bydgoszcz, Poland*
[3]*Institute of Physics, Faculty of Physics, Astronomy and Informatics, Nicolaus Copernicus University in Toruń,*
ul. Grudziądzka 5, 87-100 Toruń, Poland
[4]*Department of Physics, University of Nevada, Reno, Nevada 89557, USA*

We report numerically exact quantum scattering calculations on magnetic Feshbach resonances in ultracold, strongly anisotropic atom-molecule [Rb(^2S) + SrF($^2\Sigma^+$)] collisions based on state-of-the-art *ab initio* potential energy surfaces. We find broad resonances mediated by the intermolecular spin-exchange interaction, as well as narrow resonances due to the intramolecular spin-rotation interaction, which are unique to atom-molecule collisions. Remarkably, the density of resonances in atom-molecule collisions is not much higher than that in atomic collisions despite the presence of a dense manifold of molecular rotational states, which can be rationalized by analyzing the adiabatic states of the collision complex.

Introduction. Magnetic Feshbach resonances (MFRs) are a powerful tool to control interatomic interactions in ultracold atomic gases [1,2] being at the very heart of many intriguing quantum phenomena, such as the formation of weakly bound few-body states [3,4], quantum chaos in ultracold collisions of lanthanide atoms [5,6], and the BEC-BCS crossover [1,7]. The physical mechanism responsible for MFRs relies on the coupling between the open (i.e., scattering) and closed (i.e., bound) states of the collision complex, which is greatly amplified when these states become degenerate, leading to a resonance enhancement of the scattering cross section [2]. This coupling can arise from a variety of mechanisms, ranging from short-range spin-dependent and hyperfine interactions in ultracold atomic collisions [2,5,8–10], radiative transitions [11–13], dc electric fields [14,15], off-resonant laser fields [16], and radio-frequency dressing [17–19]. On the theoretical side, MFRs are most accurately described by rigorous coupled-channel (CC) quantum scattering calculations [2], which yield numerically exact solutions of the Schrödinger equation for a given interatomic interaction potential, thus providing unbiased insights into ultracold collision physics.

While MFRs in ultracold atom-atom collisions are well understood [2], much less is known about their atom-molecule [20–24] and molecule-molecule [25] counterparts, which have recently been observed by several groups. This is due to enormous computational challenges [26,27] caused by a large number of rotational, fine, and hyperfine states coupled by strongly anisotropic interactions, which are involved in ultracold collisions of trapped molecules produced by photoassociation (such as KRb and NaK [27–30]) and laser cooling (such as SrF, CaF, and YO [31–36]). Because the computational cost of solving CC equations scales steeply with the number of molecular rotational states (N_{max}^6 [37]), their direct numerical solution rapidly becomes computationally impractical [26,27] for all but the simplest atom-molecule collisions involving weakly interacting atoms (such as He,

Mg, and N) [38–40]. Restricted basis set computations have been performed on selected systems [24,41,42] yielding useful qualitative insights into MFRs in Na + NaLi collisions [24,42]. However, numerically exact CC calculations on MFRs in ultracold atom-molecule collisions with realistic (strongly anisotropic) interactions have remained elusive due to the unresolved challenges mentioned above. At present, such calculations are limited to atom-molecule pairs, whose hyperfine structure can be neglected (e.g., by selecting fully spin-polarized initial states [43–45]), precluding theoretical insights into a growing number of experimental observations of MFRs in ultracold atom-molecule collisions [20–23] and the exploration of MFRs in new molecular systems.

Here, we report numerically exact CC calculations of MFR spectra in ultracold, strongly anisotropic atom-molecule collisions. We focus on ultracold Rb(^2S) + SrF($^2\Sigma^+$) collisions, which are experimentally relevant in several contexts. First, SrF($^2\Sigma^+$) was the first molecule to be laser cooled [31] and confined in a magneto-optical trap [32], and collisions with cotrapped Rb atoms have been proposed as a means to further cool SrF molecules by momentum-transfer collisions with ultracold alkali-metal atoms [45,46], a technique known as sympathetic cooling [43–48]. Second, ultracold collisions of closely related CaF($^2\Sigma^+$) molecules with cotrapped Rb atoms [49], and with other CaF molecules have already been observed [50] and suppressed [51] using microwave shielding. Our results could thus be verified in near-future ultracold collision experiments.

The Rb-SrF collision complex is characterized by two deep and strongly anisotropic potential energy surfaces (PESs) of singlet and triplet symmetries [52], which can couple hundreds of rotational states [45], in addition to the pronounced hyperfine structure of both SrF and Rb, causing major computational challenges, as mentioned above. Here, we address these challenges using a recently developed total rotational angular momentum (TRAM) representation [53], which enables

us to efficiently incorporate all rotational, fine, and hyperfine states of the collision partners in converged CC calculations on realistic *ab initio* PESs. Our calculated MFR spectra are dominated by broad resonances with a density of about 5 resonances per 1 kG, which should be readily observable experimentally. Our results open up the possibility of rigorous CC calculations of MFRs on a wide range of ultracold atom-molecule collisions of experimental interest.

Theory. The Hamiltonian for a $^2\Sigma$ molecule (such as SrF) colliding with a ^2S atom (such as Rb) may be written in atomic units ($\hbar = 1$) as [53,54]

$$\hat{H} = -\frac{1}{2\mu R}\frac{\partial^2}{\partial R^2}R + \frac{\hat{L}^2}{2\mu R^2} + \hat{V}_{\text{int}} + \hat{H}_{\text{mol}} + \hat{H}_{\text{at}}, \quad (1)$$

where μ is the reduced mass of the atom-molecule trimer described by the Jacobi vectors $\mathbf{R}$ (pointing from the molecule's center of mass to the atom) and $\mathbf{r}$ (joining the nuclei of the diatomic molecule), and $\hat{L}^2$ is the squared orbital angular momentum for the collision. The atom-molecule interaction is given as $\hat{V}_{\text{int}} = \sum_{S,M_S} V_S(R,\theta)|SM_S\rangle\langle SM_S| + \hat{V}_{\text{mdd}}$, where $V_S(R,\theta)$ denote the singlet ($S = 0$) and triplet ($S = 1$) adiabatic PESs (see below), and $\hat{V}_{\text{mdd}}$ is the magnetic dipole-dipole interaction. We adopt the rigid-rotor approximation by setting $r = r_e$, the equilibrium distance in SrF, which is expected to be qualitatively accurate for collisions of rigid molecules such as SrF [55]. As such, the atom-molecule PES only depends on R and θ, the angle between $\mathbf{R}$ and $\mathbf{r}$. In Eq. (1), $\hat{H}_{\text{mol}}$ describes the isolated $^2\Sigma$ molecule, $\hat{H}_{\text{mol}} = \hat{H}_{\text{mol}}^{\text{rot}} + \hat{H}_{\text{mol}}^{\text{spin}} + \hat{H}_{\text{mol}}^{\text{spin-rot}}$, where $\hat{H}_{\text{mol}}^{\text{rot}} = B_e\hat{\mathbf{N}}^2$ is the rotational Hamiltonian, B_e is the rotational constant, $\hat{\mathbf{N}}$ is the rotational angular momentum of the diatomic molecule, and $\hat{H}_{\text{mol}}^{\text{spin}} = g_S\mu_0 B\hat{S}_Z + a\hat{\mathbf{I}}\cdot\hat{\mathbf{S}}$ is the spin Hamiltonian, which accounts for the electron and nuclear spins within the molecule described by the operators $\hat{\mathbf{S}}$ and $\hat{\mathbf{I}}$ interacting with each other via the Fermi contact interaction (coupling constant a) and with an external magnetic field B directed along a space-fixed z axis. The spin-rotation interaction $\hat{H}_{\text{mol}}^{\text{spin-rot}} = \gamma_{\text{sr}}\hat{\mathbf{N}}\cdot\hat{\mathbf{S}} + \frac{c\sqrt{6}}{3}\left(\frac{4\pi}{5}\right)^{1/2}\sum_q(-1)^q Y_{2-q}(\theta_r,\phi_r)[\hat{\mathbf{I}}\otimes\hat{\mathbf{S}}]_q^{(2)}$ includes the electron spin-rotation and anisotropic hyperfine interactions, parametrized by the coupling constants γ_{sr} and c. The internal structure of atomic Rb(^2S) is described by the Hamiltonian $\hat{H}_{\text{at}} = g_S\mu_0 B\hat{S}_{az} + A_a\hat{\mathbf{I}}_a\cdot\hat{\mathbf{S}}_a$, where $\hat{\mathbf{S}}_a$ and $\hat{\mathbf{I}}_a$ are the atomic electron and nuclear spin operators, and A_a is the hyperfine constant.

To map out the spectrum of MFRs in ultracold Rb + SrF collisions, we solve the Schrödinger equation $\hat{H}|\Psi\rangle = E|\Psi\rangle$, where E is the total energy and $|\Psi\rangle$ is the scattering wave function, by expanding the wave function of the atom-molecule collision complex as $|\Psi\rangle = R^{-1}\sum_i F_i(R)|\Phi_i\rangle$, where $|\Phi_i\rangle = |(Nl)J_r M_r\rangle|n_s\rangle|n_s^{(a)}\rangle$ are the TRAM basis functions [56], which enable a computationally efficient treatment of the essential hyperfine structure of the collision partners interacting via highly anisotropic potentials in an external magnetic field [53]. Here, $|(Nl)J_r M_r\rangle$ are the eigenstates of $\hat{J}_r^2$ and $\hat{J}_z$, where $\hat{\mathbf{J}}_r = \hat{\mathbf{N}} + \hat{\mathbf{L}}$ is the TRAM of the collision complex and $\hat{J}_z$ is its projection on the field axis. The atomic and molecular spin functions are denoted by $|n_s^{(a)}\rangle$ and $|n_s\rangle$.

Unlike the total angular momentum of the collision pair, J_r is rigorously conserved even in the presence of external
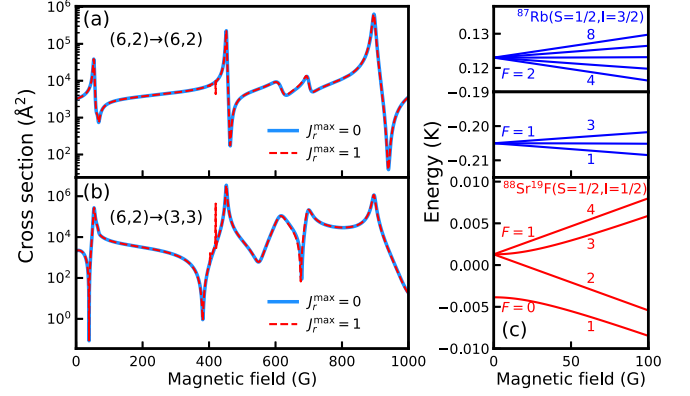

FIG. 1. Magnetic field dependence of (a) elastic and (b) inelastic cross sections for Rb($|6\rangle$) + SrF($|2\rangle$) collisions calculated with $J_r^{\max} = 0$ (solid lines) and $J_r^{\max} = 1$ (dashed lines). The collision energy is $E_c = 0.1\,\mu$K. (c) Hyperfine-Zeeman energy levels of Rb(^2S) (upper panel) and SrF($^2\Sigma^+$) (lower panel) in its ground rovibrational state.

magnetic fields and isotropic hyperfine interactions [53]. The different values of J_r can only be coupled by weak spin-rotation interactions, such as the spin-rotation and anisotropic hyperfine interactions [53]. The ensuing near conservation of J_r is key to the computational efficiency of the TRAM basis, which enables the inclusion of a sufficient number of closed rotational channels ($N_{\max} = 175$ [57]) to produce converged results for highly anisotropic Rb + SrF collisions. We integrate the CC equations numerically [58,59] to obtain the asymptotic behavior of the radial solutions $F_i(R)$, from which the S-matrix elements and scattering cross sections are obtained as a function of magnetic field [53,57].

Ab initio calculations. To describe the quantum dynamics of ultracold Rb + SrF collisions it is essential to have a realistic description of both the singlet and triplet PESs. Here, we employ the state-of-the-art *ab initio* triplet PES [45] computed using the coupled cluster method with a large basis set. To determine the singlet PES, we employ the complete active space self-consistent field (CASSCF) method using an aug-cc-pVQZ basis set and ECP28MDF core potentials for Rb and Sr [57]. The active space for this calculation includes the open-shell orbitals of both Rb and SrF, accommodating two electrons in two orbitals. The exchange energy thus obtained is added to the triplet PES [45] to produce the singlet PES. This procedure ensures the correct behavior of the singlet PES in the limit $R \to \infty$, where the exchange energy decays exponentially, and accurately accounts for dispersion interactions, which should asymptotically be identical for both the singlet and triplet PESs. We verified the correctness of the singlet-triplet energy splitting using additional spin-flip symmetry adapted perturbation theory (SAPT) calculations [60], in which the asymptotic behavior is calculated based on monomer properties [57].

Magnetic Feshbach resonances in ultracold atom-molecule collisions. We consider ultracold Rb atoms and SrF molecules colliding in the initial states $|i\rangle \otimes |j\rangle$, where $|i\rangle$ and $|j\rangle$ stand for the initial hyperfine-Zeeman states of Rb and SrF, labeled in the order of increasing energy, as shown in Fig. 1(c). In the
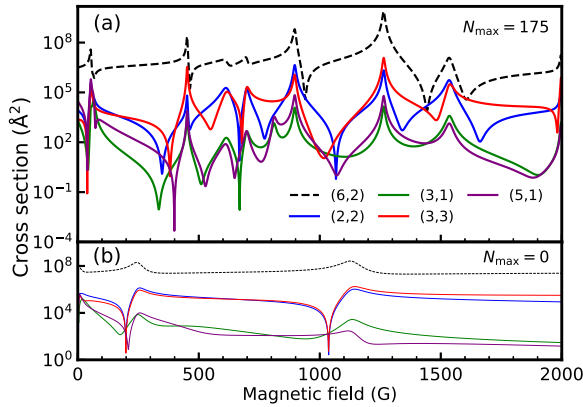
FIG. 2. (a) Calculated MFR spectra for elastic and inelastic Rb($|6\rangle$) + SrF($|2\rangle$) collisions at $E_c = 0.1\,\mu$K. The elastic cross section (black dashed line) is multiplied by 1000 for visual clarity. The final states are marked as (i, j), where i and j label the internal states of Rb and SrF [see text and Fig. 1(c)]. (b) Same as (a) but with only the $N = 0$ rotational state of SrF retained in the CC basis.

low-B-field limit, these states are identical to the atomic and molecular hyperfine states $|F_a m_{F_a}\rangle$ and $|(NSI)F m_F\rangle$, where $\hat{\mathbf{F}} = \hat{\mathbf{N}} + \hat{\mathbf{S}} + \hat{\mathbf{I}}$ is the total angular momentum of SrF, which is a vector sum of the rotational, electron spin, and nuclear spin angular momenta. We are interested in the experimentally relevant case of SrF molecules colliding in their ground rotational states ($N = 0$), which can be prepared by laser cooling and trapped in an optical dipole trap [32,35]. The hyperfine structure of SrF($N = 0$) consists of two hyperfine manifolds with $F = 1, 0$, which are split by an external magnetic field into four levels [see Fig. 1(c)]. Non-fully spin-polarized initial states of Rb and SrF can undergo collision-induced spin exchange, i.e., $|6\rangle \otimes |2\rangle \rightarrow |3\rangle \otimes |3\rangle$, which conserves the projection of the total internal angular momentum of the collision partners $m_{F_a} + m_F$. The rigorous treatment of the spin-exchange collisions and of the hyperfine structure of the collision partners constitute two key improvements over the previous calculations [45].

Figures 1(a) and 1(b) show the integral cross sections for ultracold Rb + SrF collisions as a function of magnetic field calculated with two different basis sets containing the single lowest ($J_r^{max} = 0$) and two lowest ($J_r^{max} = 1$) TRAM blocks. Both of these basis sets are converged with respect to the maximum number of rotational basis states of SrF ($N_{max} = 175$ [57]), so any difference between them quantifies the extent of TRAM conservation in ultracold Rb + SrF collisions. We observe that, save for a single narrow feature near 400 G, the cross sections calculated using the two basis sets are essentially the same across the entire magnetic field range, confirming that J_r is indeed a nearly good quantum number in Rb + SrF collisions. The broad MFRs occur due to the intermolecular spin-exchange interaction [57] (see below), and the narrow peaks can be attributed to the coupling between the different values of J_r induced by the spin-rotation interaction in SrF. We will focus on the broad MFRs obtained from $J_r^{max} = 0$ calculations.

In Fig. 2(a), we show the calculated spectrum of MFRs in ultracold Rb + SrF collisions obtained from fully converged

CC calculations with 1232 TRAM basis functions. The inelastic and elastic cross sections are comparable, which indicates that significant inelastic losses can occur near MFRs. Further work is needed to identify the parameter regimes, where these losses are suppressed. The resonance density (4–5 per 1 kG) is fairly insensitive to the initial and final hyperfine states of Rb and SrF, and is comparable to that of MFRs in ultracold Rb + Rb collisions [61]. The J_r-conserving MFRs are broad and similar to those which occur in ultracold collisions of alkali-metal atoms [2]. However, as shown below, the atom-molecule interaction anisotropy has a non-negligible effect on MFR spectra. The hyperfine structure of the collision partners and their spin-exchange interactions also play a crucial role: When the spin-exchange coupling is omitted in test calculations, most of the MFRs shown in Fig. 2(a) disappear [57].

The relatively low density of MFRs in Rb + SrF collisions is surprising, given the very large number of rovibrational and hyperfine states of the Rb-SrF collision complex that need to be included in CC calculations to produce converged results. Figure 2(b) shows a reduction in the number of MFRs when the anisotropy of the Rb-SrF interaction if turned off by setting $N_{max} \rightarrow 0$ (as done in Ref. [62]), illustrating the significant role of the anisotropic coupling between the rotational states of SrF in enhancing the density of MFRs. However, the enhancement is not dramatic. A similar observation has recently been made for MFRs in ultracold Na + NaLi collisions [24].

To further elucidate the role of anisotropic couplings between different rotational states, we diagonalized the atom-molecule Hamiltonian in Eq. (1) without the radial kinetic energy term to produce the adiabatic states of the Rb-SrF collision complex as a function of R. In the adiabatic picture, the Rb + SrF collision partners approach each other at long range on a smooth adiabatic potential, which experiences a series of avoided crossings with other potentials as R is decreased, leading to inelastic transitions and MFRs [57]. The density of the adiabatic potentials in the vicinity of the incident collision threshold is fairly well converged already for moderate values of $N_{max} \simeq 30$–60. Further increasing N_{max} only produces slight changes in the shapes of the existing adiabatic curves, leading to small changes in closed-channel bound states, which are not enough to produce new bound states that could result in additional MFRs. Therefore, the MFR density saturates at $N_{max} \simeq 30$–60 [57], well below the value required for full convergence ($N_{max} = 175$). In other words, *even though the adiabatic states themselves are not completely converged at low N_{max}, their density near the incident threshold is.* This explains why highly excited rotational states do not contribute directly to the MFR density, although they do affect the positions and widths of the individual MFRs.

It has been hypothesized that MFRs in ultracold collisions of alkali dimers with alkali-metal atoms are caused by the long-range LeRoy-Bernstein bound states [63], which are only weakly affected by the atom-molecule interaction anisotropy since it typically decreases much faster with R than the isotropic part of the PES. If this hypothesis is true, the atom-molecule MFRs would be very similar to the well-known atom-atom MFRs [2] in that the effects of short-range interaction anisotropy can be safely neglected. An opposing hypothesis states that MFRs are due to the short-range chaotic states of the atom-molecule collision complex [64,65].
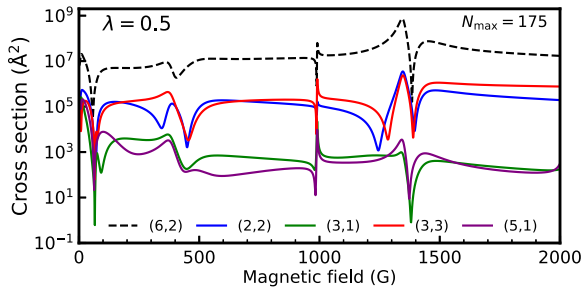
FIG. 3. Calculated MFR spectra for Rb($|6\rangle$) + SrF($|2\rangle$) collisions at $E_c = 0.1\,\mu$K with the short-range interaction PES scaled by a factor of 0.5. The elastic cross section (black dashed line) is multiplied by 1000 for visual clarity.

We emphasize that all calculations on atom-molecule MFRs reported thus far (see, e.g., [24,62]) were performed with severely restricted rotational basis sets. They were thus affected by uncontrolled basis-set truncation errors, which are absent in our calculations. For example, in the calculations of Ref. [62], only the ground rotational state was included in the basis, which amounts to neglecting the rotational structure of the molecule and the crucial anisotropy of the atom-molecule interaction at short range. Because of these drastic approximations, the previous calculations have only been able to formulate qualitative hypotheses (but not quantitative predictions) regarding the properties of atom-molecule MFRs. By contrast, our calculations treat the atom-molecule interaction anisotropy and the hyperfine structure of the collision partners exactly using converged rotational basis sets. This not only enables testing the hypotheses formulated previously, but also makes it possible to predict the properties of MFRs in atom-molecule systems with realistic interactions. Our calculations also predict a new flavor of MFR due to the intramolecular spin-rotation interaction (see Fig. 1).

To explore the short-range vs long-range character of atom-molecule MFRs, we performed additional CC calculations with the short-range part of the Rb-SrF PESs scaled by a factor of $\lambda = 0.5$ (see [57] for details). Because the long-range parts of the scaled and unscaled PESs are the same, the scaling only changes the density of short-range complex states. As a result, it should not modify the density of MFRs if, as proposed in Ref. [63], the MFRs are due to the long-range states. If, on the other hand, the MFRs are due to the short-range states, then the PES scaling is expected to lead to a substantial decrease in MFR density according to the approximate scaling $\rho \simeq (\lambda)^{3/2}$ [66]. As shown in Fig. 3, the number of MFRs decreases by 40% upon shallowing the PESs, suggesting that MFRs in Rb + SrF collisions are predominantly caused by short-range complex states. This observation does not rule out the possi-

bility that some MFRs could be caused by long-range states, which can have much narrower widths than those caused by the short-range complex states [57], warranting further calculations and experimental measurements on near-threshold bound states of Rb-SrF, whose zero-energy crossings with collision thresholds give rise to MFRs [2]. Such calculations could be enabled by combining the efficient TRAM basis used here [53] with established techniques for solving the bound-state Schrödinger equation [67].

In summary, we have presented numerically exact CC calculations of MFRs in ultracold, strongly anisotropic Rb + SrF collisions in the rigid-rotor approximation. These calculations are free from the basis set truncation errors, which affected all previous calculations on such collisions, and enable us to obtain novel insights into the properties of atom-molecule MFRs. First, we show that the MFRs can be classified into two types: (i) J_r-conserving broad resonances due to the spin-exchange splitting between the singlet and triplet PESs at short range, and (ii) narrow resonances originating from J_r-breaking intramolecular spin-rotation interactions. While the former are similar to those which occur in alkali-metal atom collisions [2], the latter are unique to atom-molecule collisions. Second, we find that the density of MFRs in Rb + SrF collisions is comparable to that in collisions of ultracold alkali-metal atoms. We explain this surprising result in terms of the density of the adiabatic states of the atom-molecule collision complex, which does not increase substantially as new rotational states are added to the CC basis. The highly excited rotational states merely affect the shape of these adiabatic potentials rather than changing their density, thereby leaving the density of MFRs unaffected. We also find that the MFRs are predominantly due to the short-range complex states, supporting the hypothesis of Refs. [64,65], although the existence of long-range complex states [63] cannot be completely ruled out. Our results suggest excellent prospects for numerically exact quantum scattering calculations of MFRs in ultracold highly anisotropic atom-molecule collisions, such as those probed in recent experiments [22,23] paving the way for future exploration of this exciting frontier of ultracold molecular physics.

[1] I. Bloch, J. Dalibard, and W. Zwerger, Many-body physics with ultracold gases, Rev. Mod. Phys. **80**, 885 (2008).

[2] C. Chin, R. Grimm, P. Julienne, and E. Tiesinga, Feshbach resonances in ultracold gases, Rev. Mod. Phys. **82**, 1225 (2010).

[3] T. Köhler, K. Góral, and P. S. Julienne, Production of cold molecules via magnetically tunable Feshbach resonances, Rev. Mod. Phys. **78**, 1311 (2006).

[4] C. H. Greene, P. Giannakeas, and J. Pérez-Ríos, Universal few-body physics and cluster formation, Rev. Mod. Phys. **89**, 035006 (2017).

[5] A. Frisch, M. Mark, K. Aikawa, F. Ferlaino, J. L. Bohn, C. Makrides, A. Petrov, and S. Kotochigova, Quantum chaos in ultracold collisions of gas-phase erbium atoms, Nature (London) **507**, 475 (2014).

[6] T. Maier, H. Kadau, M. Schmitt, M. Wenzel, I. Ferrier-Barbut, T. Pfau, A. Frisch, S. Baier, K. Aikawa, L. Chomaz, M. J. Mark, F. Ferlaino, C. Makrides, E. Tiesinga, A. Petrov, and S. Kotochigova, Emergence of chaotic scattering in ultracold Er and Dy, Phys. Rev. X **5**, 041029 (2015).

[7] C. Gross and I. Bloch, Quantum simulations with ultracold atoms in optical lattices, Science **357**, 995 (2017).

[8] D. A. Brue and J. M. Hutson, Magnetically tunable Feshbach resonances in ultracold Li-Yb mixtures, Phys. Rev. Lett. **108**, 043201 (2012).

[9] V. Barbé, A. Ciamei, B. Pasquiou, L. Reichsöllner, F. Schreck, P. S. Żuchowski, and J. M. Hutson, Observation of Feshbach resonances between alkali and closed-shell atoms, Nat. Phys. **14**, 881 (2018).

[10] C. Makrides, M. Li, E. Tiesinga, and S. Kotochigova, Fractal universality in near-threshold magnetic lanthanide dimers, Sci. Adv. **4**, eaap8308 (2018).

[11] P. O. Fedichev, Y. Kagan, G. V. Shlyapnikov, and J. T. M. Walraven, Influence of nearly resonant light on the scattering length in low-temperature atomic gases, Phys. Rev. Lett. **77**, 2913 (1996).

[12] J. L. Bohn and P. S. Julienne, Prospects for influencing scattering lengths with far-off-resonant light, Phys. Rev. A **56**, 1486 (1997).

[13] A. Devolder, E. Luc-Koenig, O. Atabek, M. Desouter-Lecomte, and O. Dulieu, Laser-assisted self-induced Feshbach resonance for controlling heteronuclear quantum gas mixtures, Phys. Rev. A **100**, 052703 (2019).

[14] M. Marinescu and L. You, Controlling atom-atom interaction at ultralow temperatures by dc electric fields, Phys. Rev. Lett. **81**, 4596 (1998).

[15] R. V. Krems, Controlling collisions of ultracold atoms with dc electric fields, Phys. Rev. Lett. **96**, 123202 (2006).

[16] A. Crubellier, R. González-Férez, C. P. Koch, and E. Luc-Koenig, Controlling the s-wave scattering length with non-resonant light: Predictions of an asymptotic model, Phys. Rev. A **95**, 023405 (2017).

[17] A. M. Kaufman, R. P. Anderson, T. M. Hanna, E. Tiesinga, P. S. Julienne, and D. S. Hall, Radio-frequency dressing of multiple Feshbach resonances, Phys. Rev. A **80**, 050701(R) (2009).

[18] T. V. Tscherbul, T. Calarco, I. Lesanovsky, R. V. Krems, A. Dalgarno, and J. Schmiedmayer, rf-field-induced Feshbach resonances, Phys. Rev. A **81**, 050701(R) (2010).

[19] D. J. Papoular, G. V. Shlyapnikov, and J. Dalibard, Microwave-induced Fano-Feshbach resonances, Phys. Rev. A **81**, 041603(R) (2010).

[20] H. Yang, D.-C. Zhang, L. Liu, Y.-X. Liu, J. Nan, B. Zhao, and J.-W. Pan, Observation of magnetically tunable Feshbach resonances in ultracold $^{23}Na^{40}K+^{40}K$ collisions, Science **363**, 261 (2019).

[21] Z. Su, H. Yang, J. Cao, X.-Y. Wang, J. Rui, B. Zhao, and J.-W. Pan, Resonant control of elastic collisions between $^{23}Na^{40}K$ molecules and ^{40}K atoms, Phys. Rev. Lett. **129**, 033401 (2022).

[22] H. Son, J. J. Park, Y.-K. Lu, A. O. Jamison, T. Karman, and W. Ketterle, Control of reactive collisions by quantum interference, Science **375**, 1006 (2022).

[23] J. J. Park, H. Son, Y.-K. Lu, T. Karman, M. Gronowski, M. Tomza, A. O. Jamison, and W. Ketterle, Spectrum of Feshbach

[24] T. Karman, M. Gronowski, M. Tomza, J. J. Park, H. Son, Y.-K. Lu, A. O. Jamison, and W. Ketterle, *Ab initio* calculation of the spectrum of Feshbach resonances in NaLi + Na collisions, Phys. Rev. A **108**, 023309 (2023).

[25] J. J. Park, Y.-K. Lu, A. O. Jamison, T. V. Tscherbul, and W. Ketterle, A Feshbach resonance in collisions between triplet ground-state molecules, Nature (London) **614**, 54 (2023).

[26] M. Morita, R. V. Krems, and T. V. Tscherbul, Universal probability distributions of scattering observables in ultracold molecular collisions, Phys. Rev. Lett. **123**, 013401 (2019).

[27] R. Bause, A. Christianen, A. Schindewolf, I. Bloch, and X.-Y. Luo, Ultracold sticky collisions: Theoretical and experimental status, J. Phys. Chem. A **127**, 729 (2023).

[28] K. K. Ni, S. Ospelkaus, M. H. G. de Miranda, A. Pe'er, B. Neyenhuis, J. J. Zirbel, S. Kotochigova, P. S. Julienne, D. S. Jin, and J. Ye, A high phase-space-density gas of polar molecules, Science **322**, 231 (2008).

[29] J. W. Park, S. A. Will, and M. W. Zwierlein, Ultracold dipolar gas of fermionic $^{23}Na^{40}K$ molecules in their absolute ground state, Phys. Rev. Lett. **114**, 205302 (2015).

[30] J. L. Bohn, A. M. Rey, and J. Ye, Cold molecules: Progress in quantum engineering of chemistry and quantum matter, Science **357**, 1002 (2017).

[31] E. S. Shuman, J. F. Barry, and D. DeMille, Laser cooling of a diatomic molecule, Nature (London) **467**, 820 (2010).

[32] J. F. Barry, D. J. McCarron, E. B. Norrgard, M. H. Steinecker, and D. DeMille, Magneto-optical trapping of a diatomic molecule, Nature (London) **512**, 286 (2014).

[33] S. Truppe, H. J. Williams, M. Hambach, L. Caldwell, N. J. Fitch, E. A. Hinds, B. E. Sauer, and M. R. Tarbutt, Molecules cooled below the Doppler limit, Nat. Phys. **13**, 1173 (2017).

[34] L. Anderegg, B. L. Augenbraun, Y. Bao, S. Burchesky, L. W. Cheuk, W. Ketterle, and J. M. Doyle, Laser cooling of optically trapped molecules, Nat. Phys. **14**, 890 (2018).

[35] D. J. McCarron, M. H. Steinecker, Y. Zhu, and D. DeMille, Magnetic trapping of an ultracold gas of polar molecules, Phys. Rev. Lett. **121**, 013202 (2018).

[36] S. Ding, Y. Wu, I. A. Finneran, J. J. Burau, and J. Ye, Sub-Doppler cooling and compressed trapping of YO molecules at μK temperatures, Phys. Rev. X **10**, 021049 (2020).

[37] D. G. Truhlar, Long-standing themes in computational chemical dynamics, Comput. Phys. Commun. **84**, 78 (1994).

[38] R. V. Krems, H. R. Sadeghpour, A. Dalgarno, D. Zgid, J. Kłos, and G. Chałasiński, Low-temperature collisions of $NH(X^3\Sigma^-)$ molecules with He atoms in a magnetic field: An *ab initio* study, Phys. Rev. A **68**, 051401(R) (2003).

[39] W. C. Campbell, T. V. Tscherbul, H.-I. Lu, E. Tsikata, R. V. Krems, and J. M. Doyle, Mechanism of collisional spin relaxation in $^3\Sigma$ molecules, Phys. Rev. Lett. **102**, 013003 (2009).

[40] M. T. Hummon, T. V. Tscherbul, J. Kłos, H.-I. Lu, E. Tsikata, W. C. Campbell, A. Dalgarno, and J. M. Doyle, Cold N + NH collisions in a magnetic trap, Phys. Rev. Lett. **106**, 053201 (2011).

[41] A. O. G. Wallis and R. V. Krems, Magnetic Feshbach resonances in collisions of nonmagnetic closed-shell $^1\Sigma$ molecules, Phys. Rev. A **89**, 032716 (2014).

resonances in NaLi + Na collisions, Phys. Rev. X **13**, 031018 (2023).

[42] R. Hermsmeier, J. Kłos, S. Kotochigova, and T. V. Tscherbul, Quantum spin state selectivity and magnetic tuning of ultracold chemical reactions of triplet alkali-metal dimers with alkali-metal atoms, Phys. Rev. Lett. **127**, 103402 (2021).

[43] T. V. Tscherbul, J. Kłos, and A. A. Buchachenko, Ultracold spin-polarized mixtures of $^2\Sigma$ molecules with *S*-state atoms: Collisional stability and implications for sympathetic cooling, Phys. Rev. A **84**, 040701(R) (2011).

[44] M. Morita, J. Kłos, A. A. Buchachenko, and T. V. Tscherbul, Cold collisions of heavy $^2\Sigma$ molecules with alkali-metal atoms in a magnetic field: *Ab initio* analysis and prospects for sympathetic cooling of SrOH($^2\Sigma^+$) by Li(^2S), Phys. Rev. A **95**, 063421 (2017).

[45] M. Morita, M. B. Kosicki, P. S. Żuchowski, and T. V. Tscherbul, Atom-molecule collisions, spin relaxation, and sympathetic cooling in an ultracold spin-polarized Rb(^2S)$-$SrF($^2\Sigma^+$) mixture, Phys. Rev. A **98**, 042702 (2018).

[46] J. Lim, M. D. Frye, J. M. Hutson, and M. R. Tarbutt, Modeling sympathetic cooling of molecules by ultracold atoms, Phys. Rev. A **92**, 053419 (2015).

[47] M. Lara, J. L. Bohn, D. E. Potter, P. Soldan, and J. M. Hutson, Ultracold Rb-OH collisions and prospects for sympathetic cooling, Phys. Rev. Lett. **97**, 183201 (2006).

[48] C. Zhang, S. T. Rittenhouse, T. V. Tscherbul, H. R. Sadeghpour, and N. R. Hutzler, Sympathetic cooling and slowing of molecules with Rydberg atoms, Phys. Rev. Lett. **132**, 033001 (2024).

[49] S. Jurgilas, A. Chakraborty, C. J. H. Rich, L. Caldwell, H. J. Williams, N. J. Fitch, B. E. Sauer, M. D. Frye, J. M. Hutson, and M. R. Tarbutt, Collisions between ultracold molecules and atoms in a magnetic trap, Phys. Rev. Lett. **126**, 153401 (2021).

[50] L. W. Cheuk, L. Anderegg, Y. Bao, S. Burchesky, S. S. Yu, W. Ketterle, K.-K. Ni, and J. M. Doyle, Observation of collisions between two ultracold ground-state CaF molecules, Phys. Rev. Lett. **125**, 043401 (2020).

[51] L. Anderegg, S. Burchesky, Y. Bao, S. S. Yu, T. Karman, E. Chae, K.-K. Ni, W. Ketterle, and J. M. Doyle, Observation of microwave shielding of ultracold molecules, Science **373**, 779 (2021).

[52] M. B. Kosicki, D. Kedziera, and P. S. Żuchowski, *Ab initio* study of chemical reactions of cold SrF and CaF molecules with alkali-metal and alkaline-earth-metal atoms: The implications for sympathetic cooling, J. Phys. Chem. A **121**, 4152 (2017).

[53] T. V. Tscherbul and J. P. D'Incao, Ultracold molecular collisions in magnetic fields: Efficient incorporation of hyperfine structure in the total rotational angular momentum representation, Phys. Rev. A **108**, 053317 (2023).

[54] R. V. Krems and A. Dalgarno, Quantum mechanical theory of atom - molecule and molecular collisions in a magnetic field: Spin depolarization, J. Chem. Phys. **120**, 2296 (2004).

[55] M. Morita, J. Kłos, and T. V. Tscherbul, Full-dimensional quantum scattering calculations on ultracold atom-molecule collisions in magnetic fields: The role of molecular vibrations, Phys. Rev. Res. **2**, 043294 (2020).

[56] A. Simoni and J. M. Launay, Ultracold atom-molecule collisions with hyperfine coupling, Laser Phys. **16**, 707 (2006).

[57] See Supplemental Material at http://link.aps.org/supplemental/10.1103/PhysRevA.110.L021301 for computational details, convergence tests, and supporting calculations.

[58] B. R. Johnson, The multichannel log-derivative method for scattering calculations, J. Comput. Phys. **13**, 445 (1973).

[59] D. E. Manolopoulos, An improved log derivative method for inelastic scattering, J. Chem. Phys. **85**, 6425 (1986).

[60] K. Patkowski, P. S. Zuchowski, and D. G. Smith, First-order symmetry-adapted perturbation theory for multiplet splittings, J. Chem. Phys. **148**, 164110 (2018).

[61] A. Marte, T. Volz, J. Schuster, S. Dürr, G. Rempe, E. G. M. van Kempen, and B. J. Verhaar, Feshbach resonances in rubidium 87: Precision measurement and analysis, Phys. Rev. Lett. **89**, 283202 (2002).

[62] R. C. Bird, M. R. Tarbutt, and J. M. Hutson, Tunable Feshbach resonances in collisions of ultracold molecules in $^2\Sigma$ states with alkali-metal atoms, Phys. Rev. Res. **5**, 023184 (2023).

[63] M. D. Frye and J. M. Hutson, Long-range states and Feshbach resonances in collisions between ultracold alkali-metal diatomic molecules and atoms, Phys. Rev. Res. **5**, 023001 (2023).

[64] M. Mayle, B. P. Ruzic, and J. L. Bohn, Statistical aspects of ultracold resonant scattering, Phys. Rev. A **85**, 062712 (2012).

[65] M. Mayle, G. Quéméner, B. P. Ruzic, and J. L. Bohn, Scattering of ultracold molecules in the highly resonant regime, Phys. Rev. A **87**, 012709 (2013).

[66] M. D. Frye and J. M. Hutson, Complexes formed in collisions between ultracold alkali-metal diatomic molecules and atoms, New J. Phys. **23**, 125008 (2021).

[67] J. M. Hutson and C. R. Le Sueur, BOUND and FIELD: Programs for calculating bound states of interacting pairs of atoms and molecules, Comput. Phys. Commun. **241**, 1 (2019).